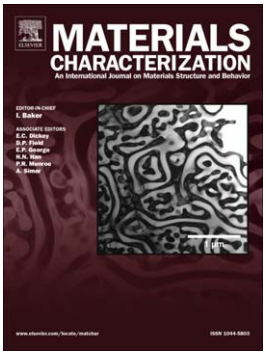

On the microstructure and texture of Cu-Cr-Zr alloy after severe plastic deformation by ECAP

Khadidja Abib, Jairo Alberto Munoz Balanos, Baya Alili, Djamel Bradai

PII: S1044-5803(15)30097-8
DOI: doi: 10.1016/j.matchar.2015.12.026
Reference: MTL 8138

To appear in: *Materials Characterization*

Received date: 28 August 2015
Revised date: 6 November 2015
Accepted date: 18 December 2015

Please cite this article as: Abib Khadidja, Balanos Jairo Alberto Munoz, Alili Baya, Bradai Djamel, On the microstructure and texture of Cu-Cr-Zr alloy after severe plastic deformation by ECAP, *Materials Characterization* (2015), doi: 10.1016/j.matchar.2015.12.026

On the microstructure and texture of Cu-Cr-Zr alloy after severe plastic deformation by ECAP

Khadidja Abib[a], Jairo Alberto Munoz Balanos[b], Baya Alili[a*], Djamel Bradai[a]

[a] *Faculty of Physics, University of Sciences and Technology Houari Boumediène, BP 32 El-Alia, Algiers, Algeria*

[b] *Departamento de Ciencia de los Materiales e Ingeniería Metalùrgica, ETSEIB – Universidad Politècnica de Cataluña, Av. Diagonal 647, 08028 Barcelona, Spain*

*Corresponding author baya_alili@yahoo.fr

Samples of a commercial Cu-1Cr-0.1Zr (wt. %) alloy were subjected to severe plastic deformation at room temperature using equal-channel angular pressing (ECAP) up to 16 passes *via* route Bc. The microstructure and texture of the processed samples were analyzed through electron backscatter diffraction (EBSD). Most of the grains were more or less inclined in the direction of shearing (45° from the extrusion direction) and substantially refined. The deformation structure evolve**d** from elongated grains to a duplex equiaxed-elongated microstructure upon straining. The fraction of high angle boundaries **gradually** increased with the number of passes up to 70%. The texture after ECAP was mainly of ECAP shear type whose components shifted slightly from their ideal positions. A net strengthening and stabilization of the $B/\overline{B}$ components were observed.

Keywords: Equal channel angular pressing (ECAP), EBSD, Cu-Cr-Zr alloy, Microstructure, Texture.

1. Introduction

Copper and copper alloys are widely used as electrical and therma**lly** conducting materials because of their excellent thermal conductivity, resistance to corrosion, ease of fabrication as well as good strength and fatigue resistance [1, 2]. Moreover, optimum resistance/conductivity values can be achieved through suitable heat treatments [3].

Severe plastic deformation (SPD) methods can generate ultrafine grained bulk materials that offer extraordinary properties, such as simultaneous ultra-high strength and high ductility [4]. SPD often carried out by equal-channel angular pressing (ECAP), has been extensively applied over the last decade on a wide variety of metals and alloys [5, 6], including pure Cu [7, 8], Cu-Cr [9-11] and Cu-Cr-Zr alloys [12].

ECAP processing **is** capable of refining the grain dimension below 1 mm as **shown** by Iwahashi *et al.* [13]. There are generally four different routes. In route A, no rotation is provided to the specimen between subsequent passes along its longitudinal axis. In contrast, the specimen is rotated by 90° in alternative directions in route B_A and in the same direction in route B_C between each passes. Finally, in route C, the sample is rotated by 180° in the same direction between subsequent passes. Route Bc has been established as the most effective way for producing an equiaxed microstructure [14–17] even if controversial results have been reported [18].

The texture evolution during ECAP strongly depends on the processing routes. Venkatachalam et al. [19] reported that the texture developed for aluminum alloy in route A was stronger than in the other processing routes due to the monotonic nature of strain path for this route. The texture resulting from ECAP following these four routes is governed by three factors**:** the applied deformation (which depends on the die configuration (Φ) and the number of passes (N)), the deformation mechanism (slip and twinning systems) and the initial texture.

Numerous works have dealt with the texture and microstructure analysis of pure Cu after severe plastic deformation [20]. To our knowledge, the texture evolution of Cu-Cr-Zr alloy during ECAP processing using route Bc has never been reported in the literature. Indeed, only studies dealing with the microstructure, electrical properties and thermal stability have been undertaken [12].

In this work, the effect of severe plastic deformation by ECAP processing using route Bc on the microstructural and textural changes of Cu-1Cr-0.1Zr (wt. %) alloy is analyzed through Electron Backscatter Diffraction (EBSD). The Vickers microhardness test was used to investigate the mechanical properties of ECAP processed samples.

2. Materials and experiments

Cu-1Cr-0.1Zr (wt. %) alloy samples (Goodfellow) of 10 mm diameter and 60 mm length were first solution annealed at 1040 °C under inert atmosphere (Argon) during 1 hour. Subsequently, they were subjected to severe plastic deformation at room temperature using the ECAP technique with a die angle of 90° and outer arc of 37° up to 16 passes following route B_c (sample rotation of 90° along its longitudinal axis in the same direction after each pass).

The extrusion rate was 0.02 m/s and molybdenum disulphide was used as lubricant. The samples for EBSD (slices of 1 mm thickness) were cut near the center of the ECAP billets (perpendicularly to the axe of the cylindrical billet in a plane parallel to the extrusion direction) and then mechanically polished with 0.02 µm colloidal silica solution. EBSD measurements were performed on the transversal plane using a Scanning Electron Microscope (SEM) with a Field Emission Gun JEOL JSM-7001F (at a 20kV voltage) using HKL Channel 5 Oxford Instruments software. The collected EBSD data enabled the determination of the mean grain size, the grain size distribution and the distribution of the boundary misorientation angles. Quantitative texture

analysis was carried out by calculating the Orientation Distribution Function (ODF) using MTex software [21]. The grain sizes were estimated from micrographs by the line intercept method.

Vickers microhardness ($Hv_{0.2}$) was measured with a load of 0.2 kg maintained for a penetration time of 20 s using a SHIMADZU type HMV-2. Five hardness indentations were randomly performed in the central areas on the sliced samples.

3. Results and discussion

3.1 Microstructure and texture before ECAP processing

3.1.1 Microstructure before ECAP processing

The microstructure of the as-received and solution annealed Cu-1Cr-0.1Zr (wt. %) alloy are shown in Fig. 1. The microstructure of the as-received alloy (Fig. 1a) is marked by a fibrous cast grain structure. It can be seen that the individual fibers are parallel elongated grains, whose major dimensions are several times longer than the transverse ones. Consequently, this reflects a columnar structure with an average transverse grain size of about 130 µm. According to Rostoker *et al.* [22], such columnar-type structure results from strong thermal gradients as expected in "chill" casting or in the fusion zone of weldments.

Fig. 1b displays the granular microstructure of the alloy obtained after solution annealing at 1040°C during 1 hour in an argon atmosphere. Grains appear nearly equiaxed with an estimated mean diameter around 100 µm. Grains seem to have irregular boundaries and high quantity of annea**ling** twin**s**.

Fig. 2 shows the grain boundary misorientation histograms of the as received and annealed Cu-1Cr-0.1Zr (wt. %) alloy at 1040°C for 1 h. It is clear that both samples do not exhibit a random distribution. The as received sample exhibits a large fraction of low angle grain boundaries (LAGBs) that may be associated with the presence of strong preferred orientations. The

histogram of misorientation angle of the solution annealed sample presents a large fraction of high angle boundaries (HAGBs) and a strong maximum near 60°, which corresponds to the Σ3 twin boundaries (60° <111>).

3.1.2 Texture before ECAP processing

Fig. 3a presents the φ_2=0 and 45° sections of the ODF of the as-received and annealed Cu-1Cr-0.1Zr (wt. %) alloy respectively. The identified texture components are also presented and their positions characteristics are given in Table 1.

The ODF sections of the as-received sample exhibit two major texture components that are Cube and a strong Copper component with a volume fraction of 13 % and 22% respectively. The Copper and cube components are usually known as the major deformation and recristallization texture components respectively observed in Cu alloys.

Fig. 3b shows that the Cube component remains but with a decreased volume fraction (10%). The Copper component disappears and a Goss component with a volume fraction of 8 % appears. It is to be noted that the origin of the Goss component, which is generally present in both deformation and recrystallization textures, is still not very clear. In the present study, the emergence of the Goss component may be explained by a rotation of the Copper component to Goss orientation. For a given material, the thermal or mechanical history, the conditions of the final anneal (the heating schedule, the furnace atmosphere, the application of stress during annealing, etc.) and the presence of minor impurities may substantially influence the annealing textures [23].

It is worth noting that the texture observed in as received and after solution annealing of Cu-1Cr-0.1Zr (wt. %) alloy is somewhat different from the recrystallization textures in FCC materials that are generated after cold and/or hot deformation [23–26]. Indeed, one has to keep in mind that the texture obtained in the present work does not correspond to the one classically observed in

FCC alloys after cold or hot deformation and recrystallization because of the fundamental difference in its thermo-mechanical history. In the present work, Cu-1Cr-0.1Zr (wt. %) alloy sample have not been subjected to any deformation prior to the solution annealing. Hence, the grains re-orientation from the columnar structure may be the result of mechanisms different from the classical ones (i.e. those governing recrystallization after hot or cold deformation).

3.2 Evolution of the microstructure and texture after ECAP processing

3.2.1 Evolution of the microstructure after ECAP processing

Fig. 4 shows the orientation imaging micrographs depicting the various microstructures of Cu-1Cr-0.1Zr (wt. %) alloy after 1, 4 and 16 ECAP passes using route Bc. The morphology of the grains is lamellar which is quite similar to the ones reported in the literature for either pure elements or alloys [27]. The grains tend to be more or less aligned, elongated and approximately inclined at 45° to the extrusion direction. As expected, the degree of refinement of the deformed microstructure increases with the number of passes but not all the grains are fully equiaxed even after 16 passes.

We have adopted the definition of the microstructural parameters for the grain size evaluation from EBSD maps used by Tirsatine *et al*. [28]. The mean grain sizes were given by the length (major axis, L) and thickness (minor axis, l) of the elongated grains.

Fig. 5 shows the evolution of these parameters as a function of the number of ECAP passes. It appears clearly that both of them decrease substantially to reach the value of L=0.73 µm and l=0.43 µm at 16 passes. No saturation is observed between 1 and 16 passes, while the value of grain aspect ratio (L/l) decrease with number of ECAP passes (from 2.14 to 1.69), indicating that grains become more or less equiaxed as the ECAP pass number increases.

Very fine and elongated microstructure in a similar alloy (Cu-0.44Cr-0.2Zr) after ECAP processing trough route Bc up to 12 passes have been reported [12, 29]. Averaged grain sizes of 160 and 200 nm were measured by these authors on TEM micrographs by the intercept method. The discrepancy with the present data of Fig. 5 may be explained by the difference in the definition of the grain size measured by EBSD and TEM techniques. In the case of EBSD map, each grain, with a certain grain tolerance angle (often less than 5°), is randomly colored, while in a TEM pattern, grain or subgrain with deformation features are directly observed. The size of the grains and/or subgrains measured on TEM micrographs are often smaller than those measured from EBSD maps.

Salimyanfard *et al.* [30] reported microstructures of copper samples subjected to severe plastic deformation by ECAP that showed a net grain refinement of both elongated and equiaxed grains. Salimyanfard *et al.* [30], Xu *et al*. [31] as well as Mishra *et al*. [32] have claimed that these small equiaxed grains have probably formed during a continuous recrystallization process as already reported in Copper and other F.C.C metals after heavy deformation at room or low temperatures [30].

Humphreys *et al*. [26] have argued that the grain refinement during ECAP could be associated with the occurrence of deformation banding that may have two possible causes. The first is related to the ambiguity associated with the selection of the operative slip systems [26]. Different lattice rotations may be generated by the selection of more than one set of slip systems in order to accommodate the steep imposed strain. The second is due to the inhomogeneous character of straining.

Histograms of the grain boundary misorientation of Cu-1Cr-0.1Zr (wt. %) alloy after 1, 4 and 16 ECAP passes using route Bc are shown in Fig. 6. It is clear that all samples do not exhibit a random distribution. It can be seen from these distributions that there was a large fraction of low-

angle boundaries in samples even after processing through 16 passes but, nevertheless, there is a gradual evolution towards higher misorientation angles with increasing numbers of passes. The large fraction of low-angle boundaries is often attributed to the continuous introduction of dislocations during repetitive processing by ECAP.

As pointed out by Humphreys *et al*. [33] the relative amount of HAGBs and LAGBs respectively as a function of deformation strain can be used to clarify the processes involved in microstructural evolution upon straining. Such data is shown in Fig. 7 where the fraction of HAGB show a continuous increase with the number of ECAP passes to reach a value of 70 % after 16 passes. This increase in the HAGB fraction can be partially attributed to special misorientation fractions with twin character. Incidentally, such evolution happened after only two passes in AA1050 and pure Cu [34, 35].

3.2.2 Evolution of the texture after ECAP processing

Fig. 8 shows the caculated ODFs from EBSD measurements of samples processed by ECAP after 1, 4 and 16 ECAP passes. The main ideal ECAP shear type texture component positions are also presented and their characteristics for FCC materials and a $\Phi = 90°$ die angle are given in Table 2 [36]. The evolution of the volume fraction of ECAP shear type texture components as function of the number of ECAP passes is shown in Fig. 9.

The texture after 1 pass is quite similar to that reported by [36, 37] for pure Copper after ECAP using route Bc, which can be represented by three fibers labeled f_1, f_2 and f_3. The f_1 fiber (referred as A_1^*- A/$\overline{A}$- A_2^*{111} partial fiber) begins with A_1^* orientation and passes through A/$\overline{A}$ (means A or $\overline{A}$) position, ends at A_2^*. The f_2 fiber starts at C, passes through $\overline{B}$/B and $\overline{A}$/A , and finishes at A_1^*. It includes then both C- $\overline{B}$/B-$\overline{A}$/A <110> partial fiber and $\overline{A}$/A-A_1^* {111} partial fiber. The f_3 fiber contains both the C- B/$\overline{B}$-A/$\overline{A}$ <110> and A/$\overline{A}$-A_2^* {111} partial fibers

[36, 37]. It can be clearly seen from Fig. 8 and Fig. 9 that all the ECAP shear components are present with a net domination of A_1^* and $\overline{A}$. After 4 passes, the texture is somewhat different to that after one pass but it still depicts main texture components along f_1-f_3 fibers as already observed by [36, 37] for pure Cu. These fibers are incomplete and a total disappearance of C A_2^* and A components is noticed. Orientation distributions are rather concentrated on A_1^*, B and $\overline{B}$ positions while for pure Cu, they were concentrated on A_1^* and C components. From Fig. 8 and Fig. 9, it is clear that the texture after the 16 passes looks very similar to that of 4 passes. The intensity and volume fraction of the A_1^* component decreases substantially and gradually from first pass to the 16th while those of B and $\overline{B}$ slightly increase and seems to saturate after 4 passes. The A_2^* and A components volume fraction decreases after 1 pass and ~~they~~ stabilize upon straining (3.8% and 3.19% respectively). The $\overline{A}$ component shows a strong decrease and also seems to stabilize.

Gazder *et al*. [38] investigated the texture evolution of pure Cu up to four ECAP passes using route Bc. They found a similar strengthening of the B and $\overline{B}$ components with concomitant C orientation deterioration. The decrease of C components was explained by its rotation along Φ by 10° in the φ_2=45°section in order to accommodate the imposed deformation [38].

The present results indicate, as already observed and discussed in the literature [39], that textures developed after ECAP following different routes (A, B_A, B_C and C), align closely along the {110} and <111> fibers. This tendency can be attributed to the large plastic strain imposed in each pass, which is sufficient to rotate a majority of the grains to the ideal ECAP orientations along these two fibers. The formation of these orientation fibers also affirms the tendency of the

crystallographic slip plane and slip direction rotate to the macroscopic shear plane and shear direct ion, respectively [39].

A more detailed analysis of the ODFs (Fig. 8) shows a slight shift, about a maximum 15°, from the ideal exact positions of the components. Such deviation, also designated as "tilts", has been already discussed [37, 40]. However, the considerable "tilts" (up to 15°) may contradict the assumption of Tóth *et al*. [41], who assumed that for a near-random texture, components very close to the ideal positions would develop. The "tilts" seem to originate from imperfect rigidity and plasticity of the material or the die geometry.

A close inspection of Figure 8 shows the absence of any new texture components, such as Cube and Goss components indicating the absence of any dynamic recrystallization process.

In order to quantitatively explain the changes in texture strength with each successive pass, the method of texture index suggested by Bunge [42] has been used. Accordingly, the index (I) of any ODF is described by an integration of the mean square of their intensity f(g) over the entire Euler space G:

$$I = \frac{1}{8\pi^2} \int_G f^2(g).dg \qquad (1)$$

It is known that the value of I increases as texture sharpens [43]. From Fig. 10, a progressive decrease of the texture index (from a value of ~ 3.2 to 1.7, indicating a relative weakening of the texture) is clearly seen. The texture index of the un-deformed initial material may also be associated with large grain size (~100 μm).

3.2.3 Evolution of Vickers microhardness

Fig. 11 **presents** the Vickers micro-hardness (H_V) as a function of number passes for route Bc. It can be seen that the first pass of ECAP process induces a significant enhancement of the micro-hardness. Then, it increases slightly and reaches the saturated value of about 170 Hv after 8 passes. The saturation reflects the lower limit of the grain size that can be achieved by ECAP as reported elsewhere [8, 30, 44]. Very similar values and trends of the micro-hardness evolution have been reported in as fabricated Cu-0.44Cr-0.2Zr (wt.%) alloy after ECAP processing *via* route Bc up to 12 passes [12]. It is also interesting to note that these values are much higher than those in pure Cu [8] and Cu-0.5Zr (wt.%) alloy [30]. It has been argued that the contributions from different strengthening mechanisms can act independently from one another and the total strength of nanostructured materials (e.g. Al alloys), can be expressed as [13, 45]:

$$\sigma = \sigma_0 + \sigma_{gs} + \sigma_{ss} + \sigma_{dis} + \sigma_{pr} \quad (2)$$

where σ_0 is the Peierls stress, σ_{gs} the grain size strengthening, σ_{ss} the solid solution hardening, σ_{dis} the dislocation strengthening, and σ_{pr} the precipitation strengthening. It can be assumed for the present study that the more effective strengthening contributions upon increasing strain are the grain size and dislocations. Indeed, σ_0 and σ_{ss} can be considered as constant and σ_{pr} is practically inexistent because second phase nano-precipitation of Cr clusters and Cr_3Zr has been shown to occur at relatively high temperature (at least 450°C).

The results from Fig. 4 and Fig. 5 suggest a grain size refinement and saturation but seem to be insufficient to determine whether these trends are maintained to very large strains as observed in the literature [46].

Subtantial increase of the dislocation densities were evidenced in Cu-2.6Ni-0.5Si (%wt.)[47] alloy that is quite similar to Cu-1Cr-0.1Zr (wt.%) alloy through X-ray diffraction line profile analysis (XRDLPA) and diffrential scanning calorimetry (DSC) analysis. Quasi parabolic

evolution of the dislocation density versus the ECAP pass number was noticed without, however, any saturation as observed for pure Cu [48]. One can notice that the dislocation density values determined from XRDLPA are lower than those deduced from DSC meaurements. Furthermore, an exhaustive estimation of the evolution of dislocation density in Cu-1Cr-0.1Zr (wt.%) alloy processed by ECAP is **an** ongoing research activity by present authors.

4. Conclusions

The microstructure of Cu-1Cr-0.1Zr (wt.%) alloy processed by ECAP *via* route Bc up to 16 passes consists of elongated subgrains aligned along the shear direction and do not evolve with increasing strain. The grains underwent a strong refinement, down to 0.7 and 0.4 µm for length and thickness respectively of the boundary spacing but do not saturate between 1 and 16 passes. The HAGB fraction show a continuous increase with increasing of number of ECAP passes.

The texture after ECAP is characterized by typical ECAP type texture of FCC metals, which deviate from their ideal positions. The texture does not show any trends towards randomization as the ECAP pass number increases, although a net strengthening and stabilization of the $B/\overline{B}$-components is observed.

The ECAP processing of Cu-1Cr-0.1Zr (wt.%) alloy *via* route Bc induces a significant enhancement of the micro-hardness up to 250%.

Acknowledgements

The authors wish to heartily thank Pr. Jose Maria CABRERA from Polytecnia ETSEIB, Universidad Politécnica de Cataluña, for inviting and helping Miss K. ABIB during her several scientific stays, Miss Ana Hernandez from Fundación CTM Centre Tecnològic, Av. de les Bases

de Manresa (Barcelona), Cataluña, for her kind assistance and Pr. Abderrahmane Si AHMED from Aix-Marseille University (IM2NP) for the improvement of the manuscript.

References

[1] MJ Tenwick and HA. Davies *Materials Science and Technology*. 1998; 98:543.

[2] DJ Edwards, BN Singh and S. Tahtinen *J Nucl Mater*. 904 (2007) 367-370.

[3] I Saglam, D Özyurek and K. Çetinkaya Effect of ageing treatment on wear properties and electrical conductivity of Cu–Cr–Zr alloy. *Bull Mater Sci*. 34(7) (2011) 1465–1470.

[4] RZ Valiev, IV Islamgaliev and IV Alexandrov. Bulk nanostructured materials from severe plastic deformation *Prog Mater Sci*. 45 (2000) 103 –189.

[5] R Valiev and TG. Langdon Principles of ECAP as a processing tool for grain refinement. *Progress in Materials Science*. 51 (2006) 881-981.

[6] AP Zhilyaev and TG. Langdon, Using high-pressure torsion for metal processing: Fundamentals and applications. *Prog Mater Sci*. 53(6) (2008) 893–979.

[7] MH Shih, CY Yu, PW Kao and CP Chang. Microstructure and flow stress of copper deformed to large plastic strains. *Scripta Mater*. 45 (2001) 793-799.

[8] A Mishra, BK Kad, F Gregori and MA. Meyers Microstructural evolution in copper subjected to severe plastic deformation: Experiments and analysis. *Acta Mater*. 55 (2007) 13 –28.

[9] A Vinogradov, T Ishida, K Kitagawa and VI. Kopylov Effect of strain path on structure and mechanical behavior of ultra-fine grain Cu–Cr alloy produced by equal-channel angular pressing, *Acta Mate*rialia. 53 (8) (2005) 2181-2192.

[10] CZ Xu, QJ Wang, MS Zheng, JW Zhu, JD Li, MQ Huang, Q.M. Jia, Z.Z. Du. Microstructure and properties of ultra-fine grain Cu-Cr alloy prepared by equal-channel angular pressing.*Mater Sci Eng*. A 459(1) (2007) 303-308.

[11] KX Wei, W Wei, F Wang, QB Du, IV Alexandrov and J. Hu. Microstructure, mechanical properties and electrical conductivity of industrial Cu-0.5%Cr alloy processed by severe plastic deformation. J. *Mater Sci Eng*. A. 528(3) (2011) 1478-1484.

[12] A Vinogradov, V Patlan, Y Suzuki, K Kitagawa and VI Kopylov. Structure and properties of ultra-fine grain Cu–Cr–Zr alloy produced by equal-channel angular pressing. *Acta Mater*. 50 (2002) 1639–1651.

[13] Y Iwahashi, Z Horita, M Nemoto, TG. Langdon The Process of Grain Refinement in Equal-Channel Angular Pressing. *Acta Materialia* . 46 (1998) 3317–3331.

[14] TG Langdon, M Furukawa, M Nemoto and Z. Horito Using equal-channel angular pressing for refining grain size. *J Organomet Chem*. 52 (2000) 30-33.

[15] Y Iwahashi, Z Horito, M Nemoto and TG. Langdon The process of grain refinement in equal-channel angular pressing. *Acta Mater*. 46 (1998) 3317−3331.

[16] K Ohi-Shi, Z Horito, M Furukawa, M Nemoto and TG. Langdon Optimizing the Rotation Conditions for Grain Refinement in Equal-Channel Angular Pressing. *Metall Mater Trans*. A 29 (1998) 2011-2013.

[17] Y Iwahashi, Z Horito, M Nemoto and TG. Langdon An investigation of microstructural evolution during equal-channel angular pressing. *Acta Mater*. 46 (1997) 4733-34741.

[18] PB Prangnell, A Gholinia and VM Markushev. In: *Investigations and Applications of Severe Plastic Deformation* (2000); (Kluwer Academic Publications, Dordrecht).

[19] P Venkatachalam, S Roy, B Ravisankar, P. V.Thamos, M Vijayalakshmi and S Suwas. Effect of processing routes on evolution of texture heterogeneity in 2014 aluminium alloy

deformed by equal channel angular pressing (ECAP) *Materials Science and Technology*. 28 (12) (2012) 1445-1458.

[20] Y Estrin and A. Vinogradov Extreme grain refinement by severe plastic deformation: A wealthof challenging science. *Acta Materialia*. 61 (2013) 782 –817.

[21] F Bachmann, R Hielscher and H. Schaeben Texture Analysis with MTEX – Free and Open Source Software Toolbox. *Solid State Phenom*. 2010; 160:6 -68.

[22]W Rostoker and JR. Dvorak In: *Interpretation of Metallographic Structures*. Academic Press Inc., London, (1965) 91-64.

[23] H. Hu *Texture of metals* (Gordon and Breach Science Publishers Ltd, United Kingdom, (1974) 233-258.

[24] E Hornbogen and U. Koste In: F Haessner, Dr. Riderer ed., *Recrystallization of metallic materials* Verlag, Stuttgart, (1978)159.

[25] C Donadille, R Valle, P Dervin and R. Penelle Development of texture and microstructure during cold-rolling and annealing of f.c.c. alloys: example of an austenitic stainless steel. *Acta Metall*. 37 (1989) 1547-157.

[26] FJ Humphreys and M. Hatherly In: *Recrystallization and related annealing phenomena*. Published Amsterdam, Boston, (2004) 380.

[27] Z. Horita In: Bulk Nanostructured Materials (WILEY-VCH Verlag GmbH & Co. KGaA, Weinheim. (2009) 205-215.

[28] K Tirsatine, H Azzeddine, T Baudin, AL Helbert, F Brisset, B Alili and D. Bradai, Texture and microstructure evolution of Fe-Ni alloy after accumulative roll bonding. Journal of Alloys and Compounds. 610 (2014) 352-360.

[29] A Vinogradov, Y Suzuki, T Ishida, K Kitagawa and VI Kopylov. Effect of Chemical Composition on Structure and Propertiesof Ultrafine Grained Cu-Cr-Zr AlloysProduced by Equal-Channel Angular Pressing. *Materials Transactions*. 45(7) (2004) 2187- 2191.

[30] F Salimyanfard, M R Torpghinejad, F Ashrafizadeh, M Hoseini, JA. Szpunar Investigation of texture and mechanical properties of copper processed by new route of equal channel angular pressing. *Materials and Design.*; 44 (2013) 374–381.

[31] C Xu, M Furukawa, Z Horita and TG. Langdon Using ECAP to achieve grain refinement, precipitate fragmentation and high strain rate superplasticity in a spray-cast aluminum alloy. *Acta Mater*. 51 (2003) 6139–6148.

[32] A Mishra, V Richard, F Gregori, B Kad, RJ Asaro, MA Meyers, et al. In: Trans Tech ed., *Nanomaterials by severe plastic deformation*.: Switzerland, (2006)19–25.

[33] FJ. Humphreys Grain and subgrain characterisation by electron backscatter diffraction. *J Mat Sci*.; 36 (2001) 3833–3854.

[34] C Harris, PB Prangnell and X. Duan In Sato T. et al. ed., In : *The 6th Int. Conf on Aluminium Alloys (ICAA6)* Toyohashi, Japan, (1998) 583.

[35] OF Higuera-Cobos, JA Berrios-Ortiz, and JM. Cabrera Texture and fatigue behavior of ultrafine grained copper produced by ECAP. *Materials Science & Engineering*. A 609 (2014) 273-282.

[36] IJ Beyerlein and LS. Toth Texture evolution in ECAE. *Progress in Materials Science.* 54 (2009) 427-510.

[37] S Li, IJ Beyerlein, DJ Alexander and SC Vogel. Texture evolution during multi-pass equal channel angular extrusion of copper: Neutron diffraction characterization and polycrystal Modelling *Acta Mater*. 53 (2005) 2111−2125.

[38] AA Gazder, F Dalla Torre, CF Gu, CHJ Davies, and EV. Pereloma Microstructure and texture evolution of bcc and fcc metals subjected to equal channel angular extrusion. *Materials Science and Engineering*.; A 415 (2006) 126 –139.

[39] S Li, AA Gazder, IJ Beyerlein, EV Pereloma, CHJ. Davies *Acta Mater*.; 54 (2006) 1087–1100

[40] W Skrotzki, C Trankner, R Chulist, B Beausir, S Suwas and LS. Toth Texture heterogeneity in ECAP deformed copper. *Solid State Phenomena*.; 160, (2010) 47-54.

[41] LS Toth, R Arruffat-Massion, L Germain, SC Baik and S. Suwas Analysis of texture evolution in equal channel angular extrusion of copper using a new flow field. *Acta Materialia*.; 52(7), (2004) 1885-1898.

[42] HJ. Bunge In: *Texture Analysis in Materials Science: Mathematical Methods*, Butterworth & Co, (1982).

[43] S Suwas, R Arruffat-Massion , LS Tóth , JJ Fundenberger, A Eberhardt and W.Skrotzki Evolution of crystallographic texture during ECAE of copper: The role of material variables. *Metallurgical and Materials Transactions A*.; 37: (2006) 739-753.

[44] N Lugo, N Llotca, JJ Sunol, JM. Cabrera Thermal stability of ultrafine grains size of pure copper obtained by equal-channel angular pressing. *J Mater Sci*.; 45: (2010) 2264 –2273.

[45] TD Topping, B Ahn, Y Li, SR Nutt and EJ. Lavernia Influence of process parameters on the mechanical behavior of an ultrafine-grained Al alloy. *Metallurgical and Materials Transactions A*.; 43 (2): (2012) 505-519.

[46] R Pippan, F Wetscher, M Hafok, A Vorhauer, I. Sabirov The limits of refinement by severe plastic deformation . *Journal: Advanced Engineering Materials.* ; 8 (2006) :1046-1056.

[47] F. Hadj Larbi, K. Abib, A.Y. Khereddine, B. Alili, M. Kawasaki, D. Bradai and T.G. Langdon In: Proceedings of 22nd International Conference on Metallurgy and Materials (Metal'2013) 15-17. 5. Brno, Czech Republic, EU. (2013)

[48] T. Ungar, E. Schafler, P. Hanak, S. Bernstorff, M. Zehetbauer, *Materials Science and Engineering*. A, 462, (2007); 398-401.

Figure captions:

Fig. 1: Microstructure of Cu-1Cr-0.1Zr (wt. %) alloy: a) as received and b) annealed at 1040 °C during 1 hour.

Fig. 2: Histograms of the misorientation angles of as received and annealed Cu-1Cr-0.1Zr (wt. %) alloy at 1040 °C during 1 hour.

Fig. 3: ODF sections at φ_2= 0 and 45° of Cu-1Cr-0.1Zr (wt. %) alloy: a) as received and b) annealed at 1040 °C during 1 hour.

Fig. 4: EBSD orientation microscopy maps of Cu-1Cr-0.1Zr (wt. %) alloy after ECAP processing using route Bc: a) 1 pass, b) 4 passes and c) 16 passes.

Fig. 5: Evolution of the L and l boundary spacing of the Cu-1Cr-0.1Zr (wt. %) alloy after ECAP processing using route Bc up to 1, 4 and 16 passes.

Fig. 6: Histograms of the misorientation angles after ECAP processing using route Bc up to 1, 4 and 16 passes.

Fig. 7: Evolution of the HAGB and LAGB of Cu-1Cr-0.1Zr (wt. %) alloy after ECAP processing using route Bc up to 1, 4 and 16 passes..

Fig. 8: ODF sections at φ_2 = 0 and 45° of Cu-1Cr-0.1Zr (wt. %) alloy after ECAP processing using route Bc up to: a) 1 pass, b) 4 passes and c) 16 passes.

Fig. 9: Volume fraction of texture components versus number of ECAP passes up to 16 passes.

Fig. 10: Variation of the texture index value as a function of ECAP pass number.

Fig. 11: Vickers micro hardness of Cu-1Cr-0.1Zr (wt. %) alloy as a function of ECAP pass number.

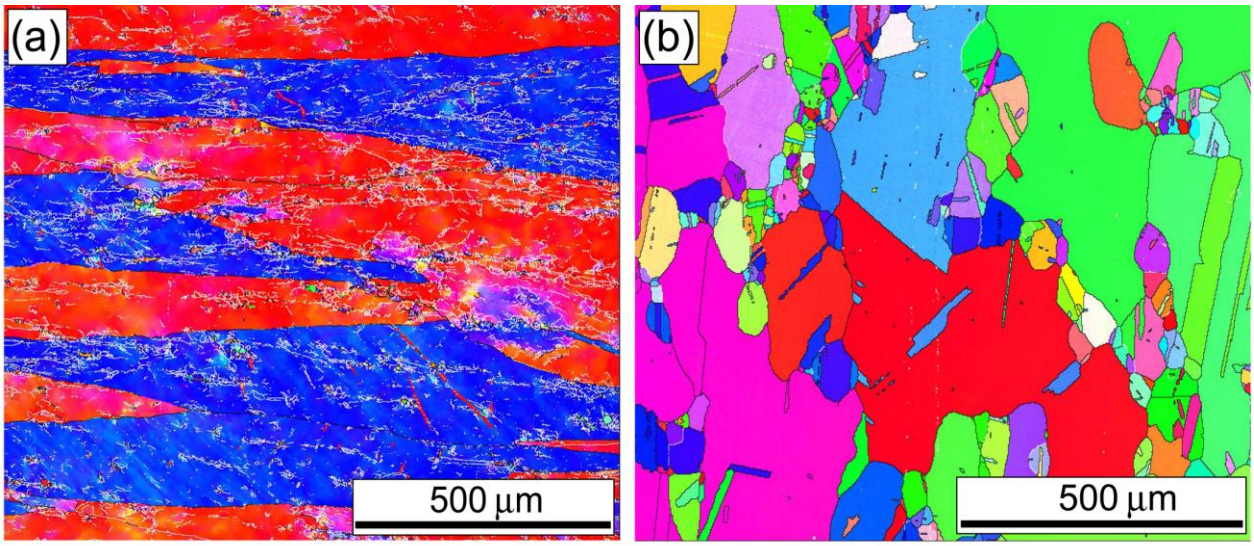

Figure 1

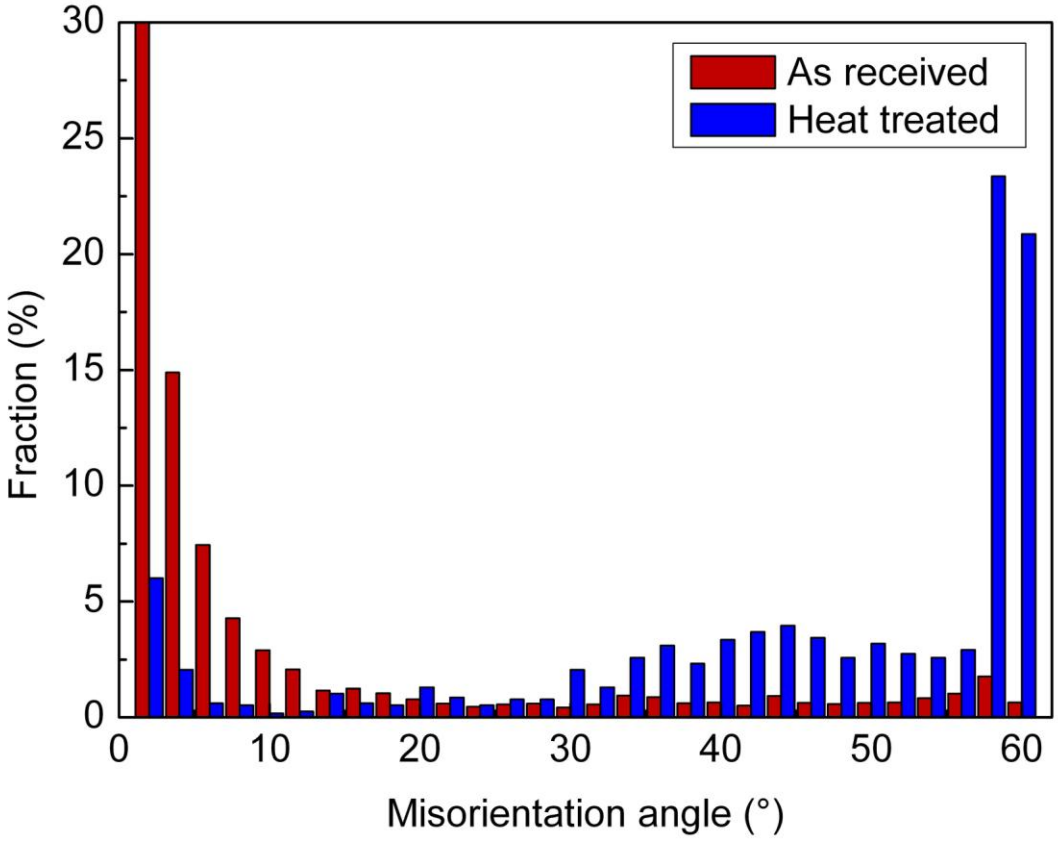

Figure 2

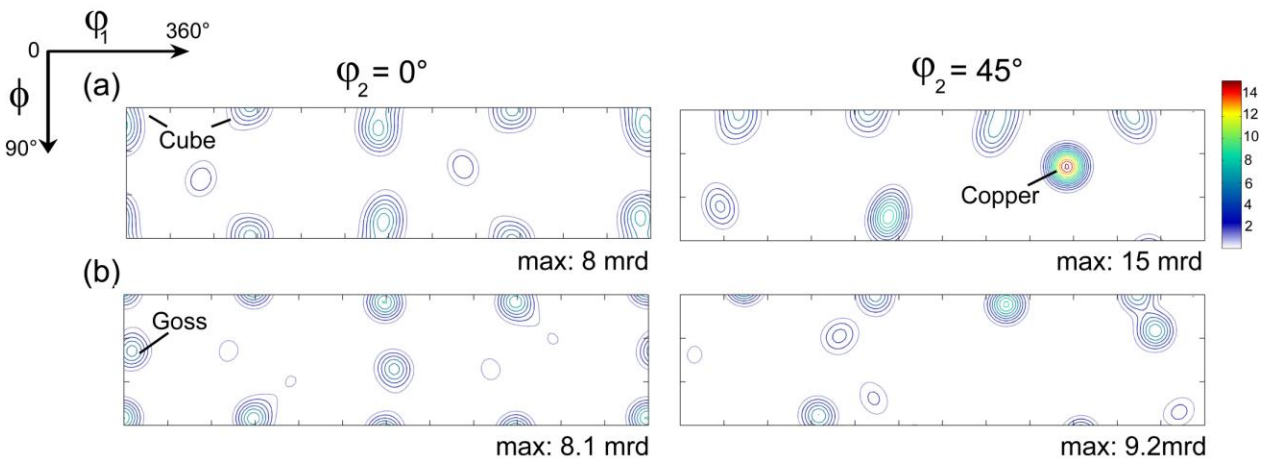

Figure 3

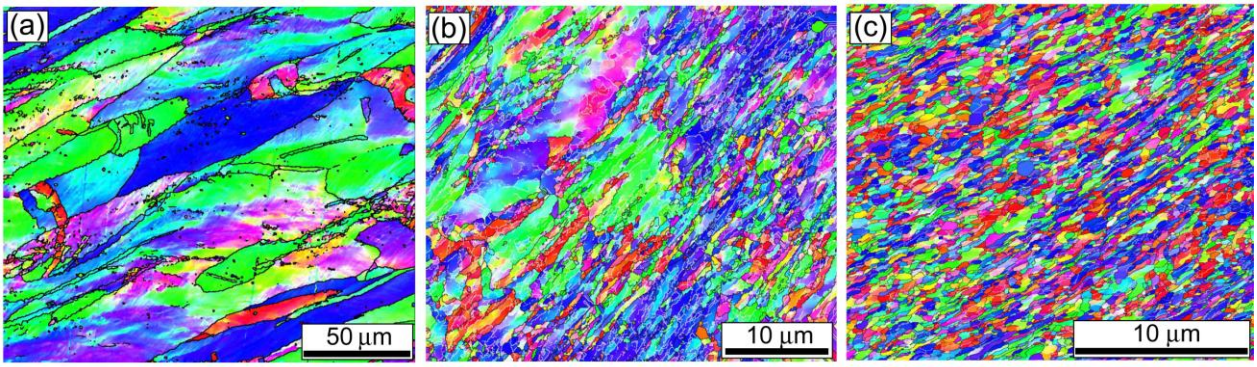

Figure 4

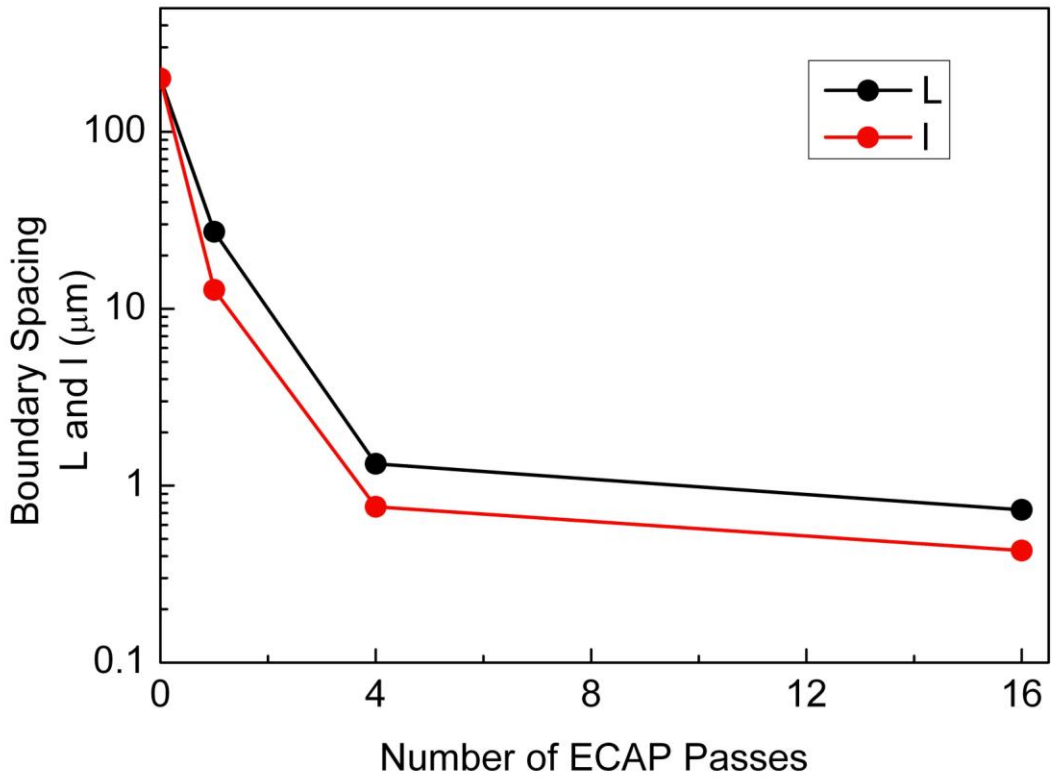

Figure 5

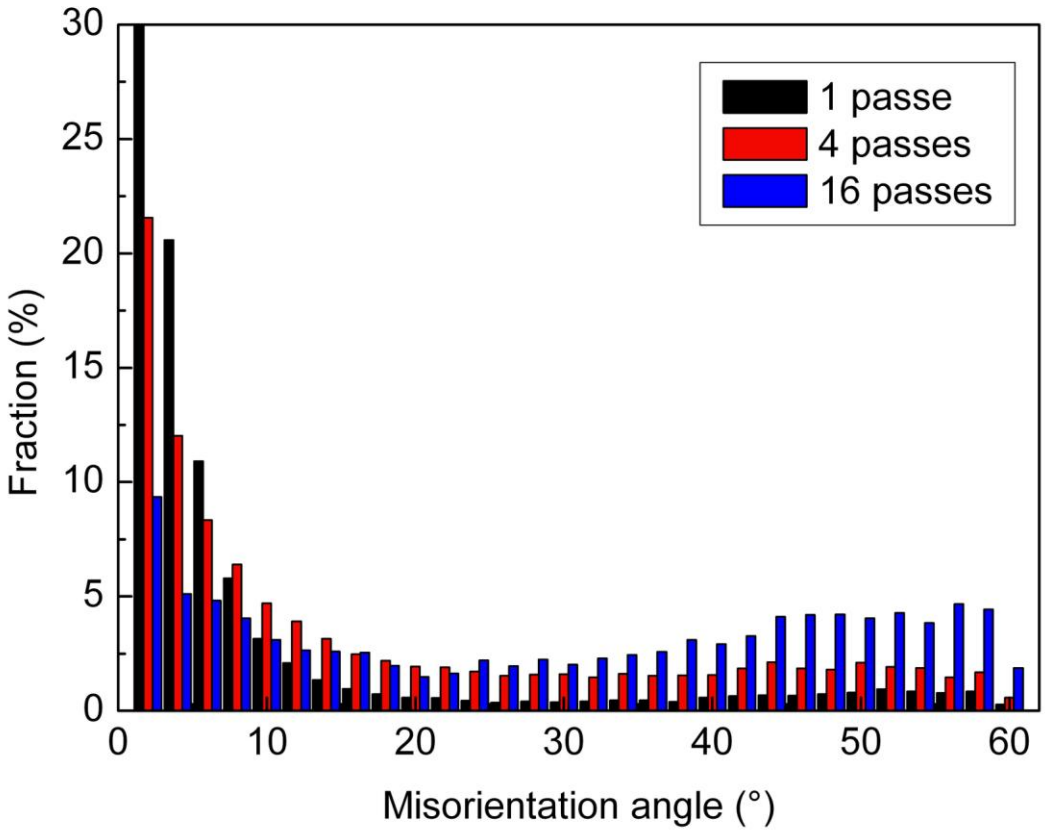

Figure 6

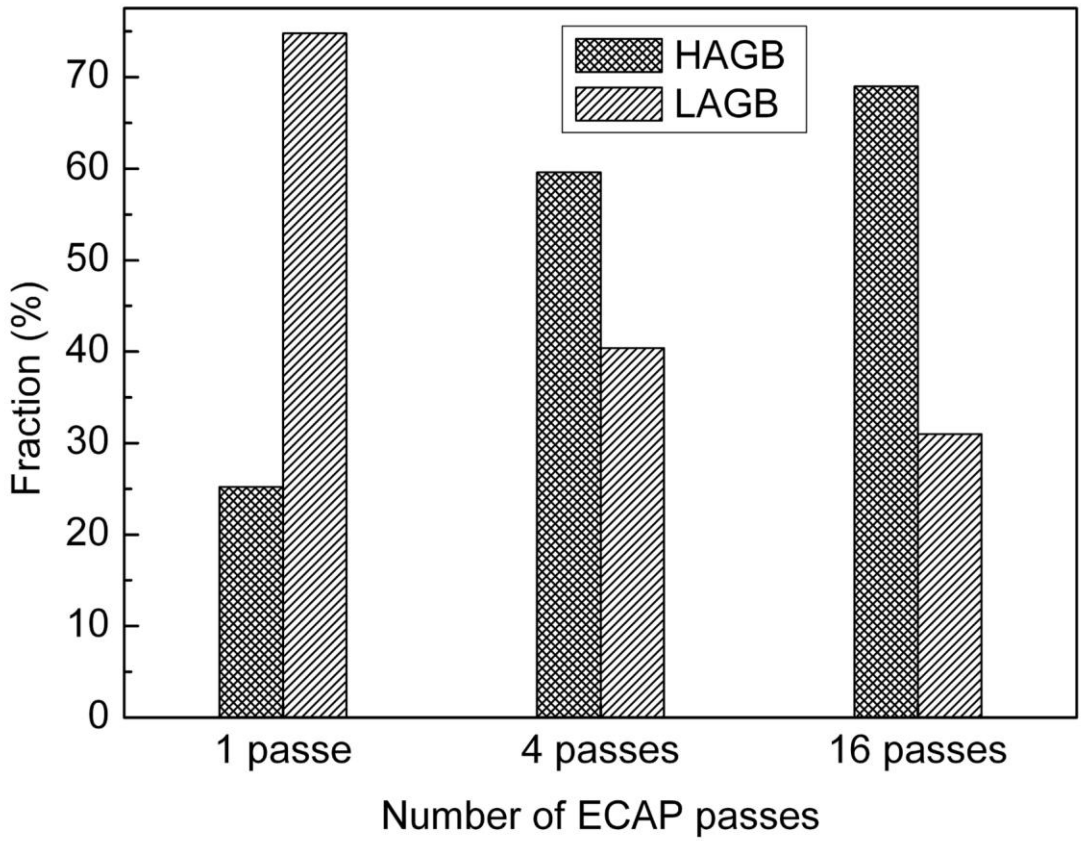

Figure 7

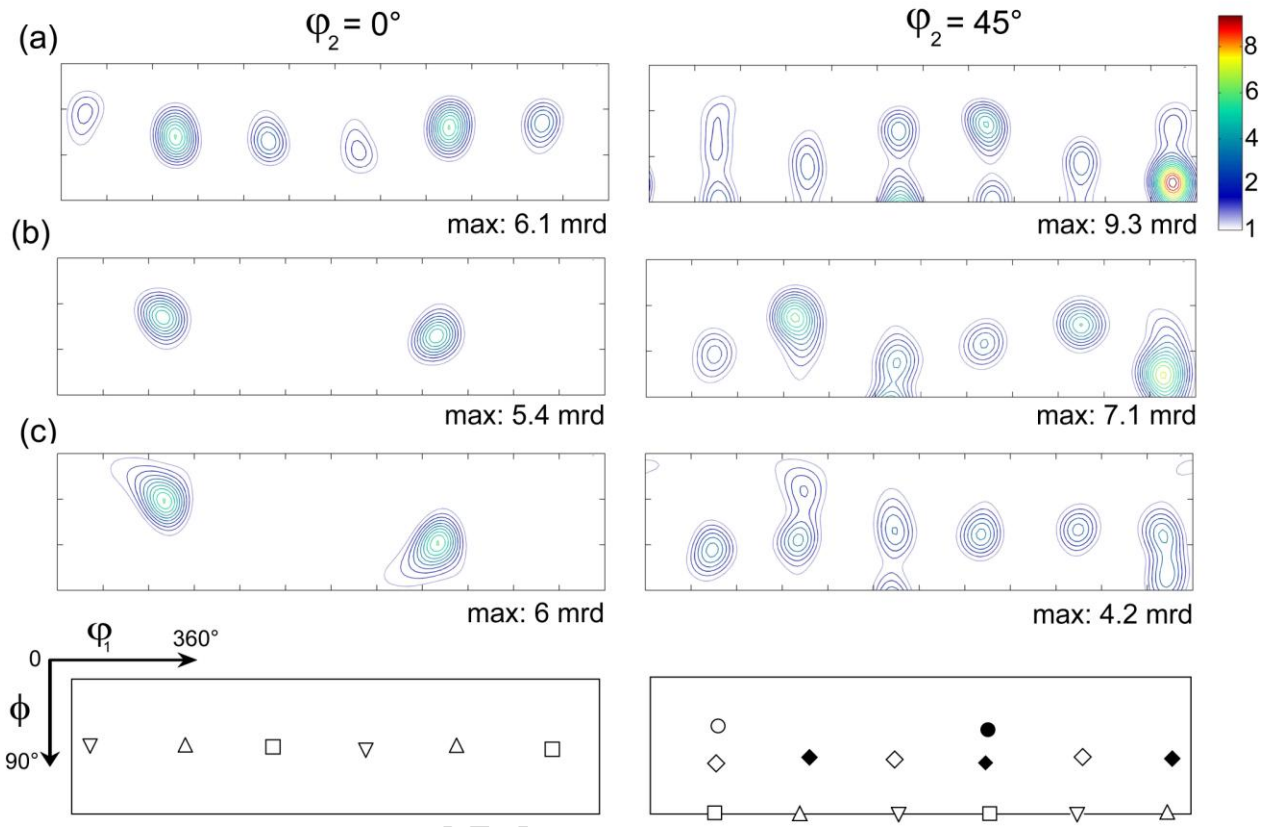

Figure 8

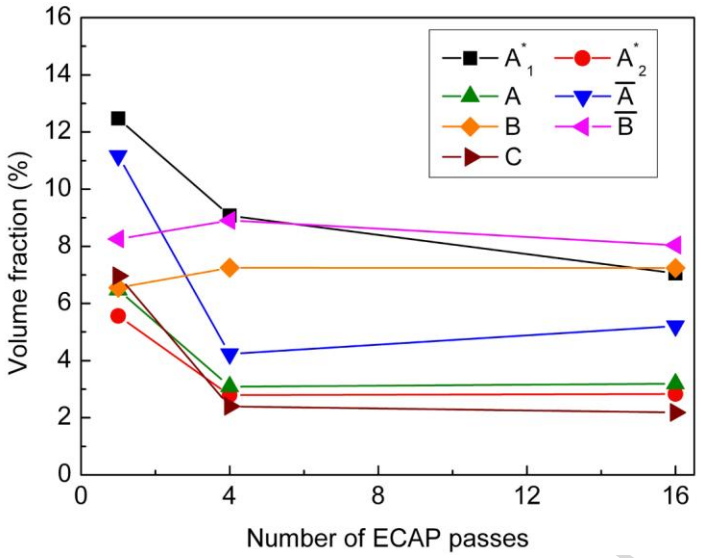

Figure 9

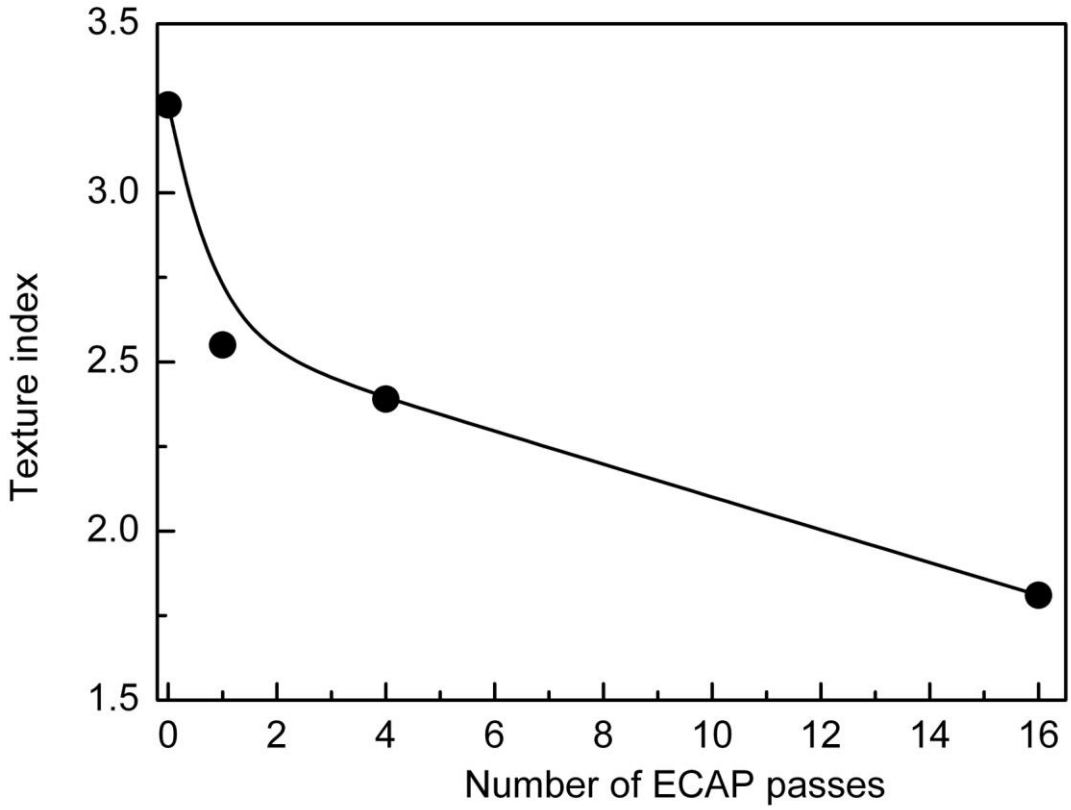

Figure 10

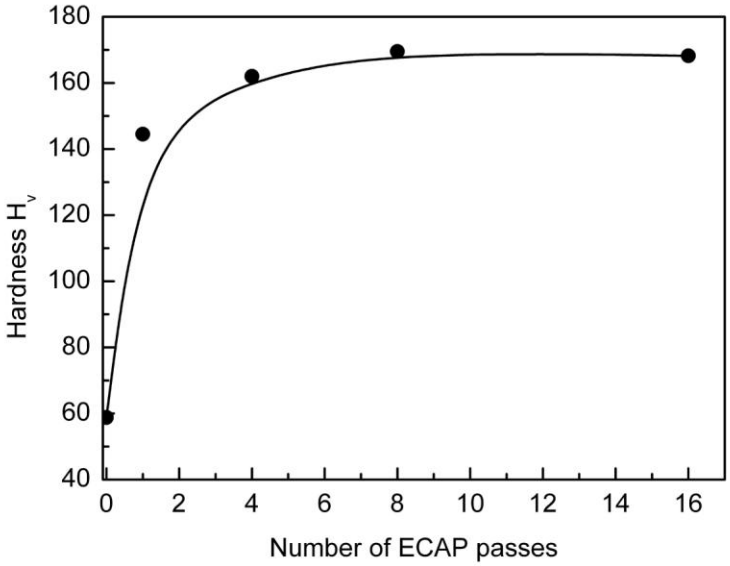

Figure 11

Table 1: Euler angles of Cube, Goss and Copper texture components.

Notation	Euler angles (°) for φ_2 = 0° and 45° sections		
	φ_1	ϕ	φ_2
Cube	0/90	0/90	0/90
Goss	0	45	0/90
Copper	270	35,26	45

Table 2 : Ideal ECAP orientations for FCC materials using a channel angle of 90°.

Notation		Euler angles (°) for φ_2 = 0° and 45° sections		
		φ_1	ϕ	φ_2
△	A_1^*	80.26/ 260,26	45	0
		170.26/ 350.26	90	45
▽	A_2^*	9.74/189.74	45	0
		99.74/279.74	90	45
○	A	45	35.26	45
●	$\overline{A}$	225	35.26	45
◇	B	45/165/285	54.74	45
◆	$\overline{B}$	105/225//345	54.74	45
□	C	135/315	45	0
		45/225	90	0

Highlights

- The microstructure consisted of elongated subgrains aligned along the shear direction.
- The subgrains underwent a strong refinement down to 0.7 μm for the major spacing.
- The texture was characterized by typical ECAP shear texture.
- A net strengthening and stabilization of the $B/\overline{B}$ texture components was observed.
- ECAP processing induced a significant enhancement of the micro-hardness up to 250%.